Chinese Chemical Letters 35 (2024) 108820

Contents lists available at ScienceDirect

Chinese Chemical Letters

journal homepage: www.elsevier.com/locate/cclet

Ba^{2+}/Ca^{2+} co-crosslinked alginate hydrogel filtration membrane with high strength, high flux and stability for dye/salt separation

Ningning Gao[a], Yue Zhang[b], Zhenhao Yang[b], Lijing Xu[b], Kongyin Zhao[b,*], Qingping Xin[b], Junkui Gao[a], Junjun Shi[a], Jin Zhong[a], Huiguo Wang[a,*]

[a] SINOPEC Research Institute of Petroleum Processing CO., LTD., Beijing 100083, China
[b] State Key Laboratory of Separation Membranes and Membrane Processes/National Centre for International Joint Research on Separation Membranes, Tiangong University, Tianjin 300387, China

ARTICLE INFO

Article history:
Received 16 November 2022
Revised 9 July 2023
Accepted 16 July 2023
Available online 20 July 2023

Keywords:
Alginate
Filtration membrane
Ba^{2+}/Ca^{2+} ion crosslinking
Dye/salt separation
Molecular dynamic simulation
Hydrogel

ABSTRACT

Alginate is a natural polysaccharide polymer. Hydrogel filtration membranes prepared from alginate show excellent fouling resistance and controllable separation performance, but poor mechanical properties limit the use of algae hydrogels. In this study, Ba^{2+}/Ca^{2+} co-crosslinked alginate (Ba/CaAlg) hydrogel membrane was prepared by cross-linking sodium alginate with a blend aqueous solution of barium ions and calcium ions, and the membrane was applied to the separation of dyes/salts from dyeing wastewater. Compared with the CaAlg membrane, the Ba/CaAlg hydrogel membrane exhibited more stable structure, and the mechanical properties and salt tolerance of the membrane were significantly improved. The flux of Ba/CaAlg membrane for methyl blue/sodium chloride mixed solution reached 43.5 L m^{-2} h^{-1}, which was significantly higher than that of CaAlg membrane. Besides, the Ba/CaAlg membrane showed higher dye rejection (>99.6%) and lower salt rejection (<8.2%). The structure of Ba/CaAlg membrane was preliminarily simulated by molecular dynamics, and the pore size and distribution of the membrane were calculated. The Ba/CaAlg membrane has a broad application prospect in dyes/salts separation.

Nanofiltration (NF) technology, due to its simple equipment, low energy consumption and high selectivity, has shown great advantages in modern industry, including seawater desalination, water purification, pharmaceuticals and biotechnology, textile industry, *etc*. [1]. Most of the current widespread applications in wastewater treatment are polymeric material based filtration membranes [2,3]. However, most of these membranes originate from non-renewable petrochemical resources. Besides, the preparation process not only involves toxic organic solvents, but also requires significant energy consumption, both of which are not conducive to sustainable development obviously [4].

Hydrogel with three-dimensional cross-linked structure is favored in the preparation of many functional materials due to their excellent hydrophilicity, flexibility and biocompatibility [5,6]. Bio-based hydrogels with rich functional groups have natural advantages. Among them, algal polysaccharides have excellent film-forming ability and have been widely used in food, pharmaceuticals, chemicals, textile printing and dyeing, and many other fields [7,8]. Sodium alginate, the most common algal polysaccharide in nature, is a linear dimeric copolymer of β-D mannuronic acid (M) and α-L guluronic acid (G), and can be further cross-linked with metal ions in an egg box structure to form a gel with three-dimensional network structure [9]. The affinity order of divalent metal ions to alginate is: $Pb^{2+} > Cu^{2+} > Cd^{2+} > Ba^{2+} > Sr^{2+} > Ca^{2+}$, with different cations binding to the blocks to form different structures [10]. Alginate hydrogel has the porous structure and exhibits excellent anti-pollution properties brought by the hydrophilic surface containing a large number of carboxyl functional groups, and has good environmental sustainability and biocompatibility. In recent years, calcium alginate has been widely studied as a membrane material, showing excellent pollution resistance and controllable separation performance [11,12]. However, the inherent drawbacks of CaAlg membranes, including poor mechanical strength, low flux and, in particular, swelling in monovalent salt solutions, limit its industrial application.

The methodologies of introducing porous carrier [13], blending modification [12] and crosslinking [14,15] were used to improve the swelling of alginate hydrogels, and to adjust the permeability of alginate membranes, thus broadening the application scope of alginate membranes. Xie *et al*. prepared hydrogel mem-

* Corresponding authors.
E-mail addresses: zhaokongyin@tjpu.edu.cn (K. Zhao), wanghg.ripp@sinopec.com (H. Wang).

https://doi.org/10.1016/j.cclet.2023.108820
1001-8417/

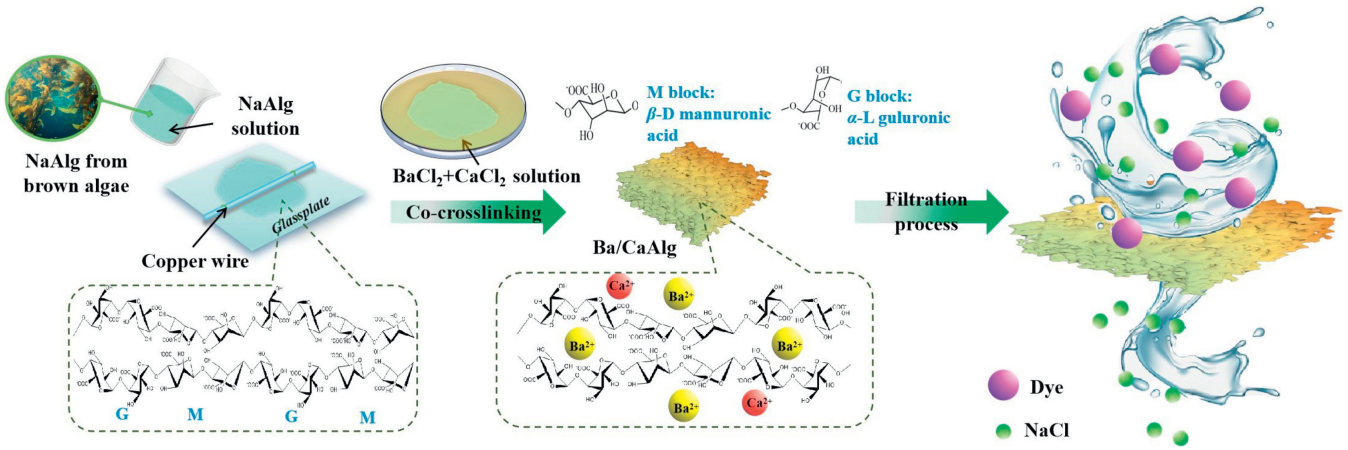

Fig. 1. Schematic diagram for the preparation of Ba/CaAlg membrane and the dye/salt separation process.

brane that can resist high concentration salt swelling by crosslinking sodium alginate and carboxymethyl chitosan with oxalic acid instead of metal ions, which could be used for dye/salt separation [16]. Gao *et al.* crosslinked NaAlg with Cu^{2+} to form self-assemble CuAlg hydrogel layer by layer on the polymer basement membrane, and the obtained membrane exhibited excellent durability under high acid and alkali conditions in crude oil/water separation [17]. Compared with Cu^{2+}, Ba^{2+} cross-linked alginate hydrogel displays better biocompatibility and has been widely used in the biological field [6,18]. Compared with Ca^{2+}, hydrogels crosslinked with Ba^{2+} have higher crosslinking density, lower water content, denser internal structure and higher Young's modulus [19].

Since water treatment needs to minimize the impact on the biological environment, Ba^{2+} crosslinked alginate with low toxicity should be selected. In addition, considering the different binding modes of Ca^{2+} and Ba^{2+} with different alginate blocks, Ca^{2+} binds to G and MG segments, while Ba^{2+} binds to G and M segments [20]. In this work, Ba^{2+} and Ca^{2+} were used as crosslinker to achieve crosslinking of all GG, MM and MG segments to endow the membrane with a more stable hydrogel structure (Ba/CaAlg). The stability, durability and dye/salt separation performance of the membrane were tested. And the structure of Ba/CaAlg membrane was studied by molecular dynamics (MD) simulation, which provided a theoretical basis for practical application. The preparation procedure of Ba/CaAlg membrane is shown in Fig. 1. The NaAlg solution with a concentration of 2.5 wt% was prepared and defoamed. Then the mixed solution of $BaCl_2$ and $CaCl_2$ with a total concentration of 2.5 wt% was prepared. The thickness of the membrane was controlled by winding copper wires with a diameter of 0.5 mm at both ends of the glass rod. The NaAlg solution was uniformly coated on a clean glass plate with a glass rod, and quickly immersed in a mixed solution of $BaCl_2$ and $CaCl_2$ for 8 h to obtain Ba/CaAlg membrane. The membranes were named according to the ratio of Ba/Ca. The membrane prepared by the molar ratio of Ba^{2+}:Ca^{2+} = 1:9 was named Ba/CaAlg-1/9.

The microscopic morphology of the surface and cross-section of the Ba/CaAlg membrane was observed by scanning electron microscopy. As shown in Figs. 2a and b, the hydrogel layer on the surface of the Ba/CaAlg membrane is uniform and dense, with a small number of crystalline particles attached to the membrane surface. Some researchers [21,22] have also observed similar phenomena and attributed them to the following three reasons: (i) Ba^{2+} has larger size and slower diffusion rate than Ca^{2+}. There are still some Ba^{2+} that fail to diffuse through the membrane body before complete crosslinking of the surface occurred. (ii) The Ba^{2+} is expected to occupy a larger space between alginate molecules, leaving smaller voids, so the process of Ba^{2+} entering the gel network is more difficult than that of Ca^{2+}. (iii) The solubility of $BaCl_2$ in water is lower than that of $CaCl_2$ and may precipitate as crystals on the membrane surface during drying. It can be found from the cross-section electron microscopy images that the Ba/CaAlg membrane is uniform and has no finger-like pore structure. The atomic force microscope (AFM) three-dimensional image in Fig. 2c also shows that the surface roughness of Ba/CaAlg membrane was larger than that of traditional pure alginate hydrogel membrane [12], consistent with the observation in the electron microscope (SEM) image.

Membranes need to have sufficient strength as well as resistance to deformation to withstand the external forces exerted during the driving process of separation. Therefore, we investigated the effect of the crosslinker [Ba^{2+}:Ca^{2+}] ratio on the mechanical properties of the formed Ba/CaAlg hydrogels, and compared with the pure CaAlg membrane. The stress-strain curves of the membranes are shown in Fig. 2d. As the [Ba^{2+}:Ca^{2+}] ratio increases, the fracture strength of the membranes gradually increases and the elongation at break gradually decreases. This is due to the fact that alginate will form a stronger hydrogel in the presence of Ba^{2+}. Furthermore, Ba^{2+} and Ca^{2+} can cross-link GG, MM, and MG segments of alginate, a structure with higher stability [20]. The membrane with the highest breaking strength was Ba/CaAlg-1/1, which reached 2.47 MPa. However, too high Ba^{2+} crosslinking concentrations in turn lead to high hardness and low toughness of the hydrogel [23].

The swelling ratios of Ba/CaAlg membranes with different [Ba^{2+}:Ca^{2+}] ratios were compared after 2 h in 5.0 g/L NaCl. As shown in Fig. 2e, the Ba/CaAlg membranes did not break after long time immersion in NaCl solution and the swelling rate did not exceed 80%, due to the co-crosslinking structure of the hydrogel. The equilibrium swelling rate of Ba/CaAlg-1/1 was 31.2%, and the most stable hydrogel network structure was formed with the lowest swelling rate.

The surface hydrophilicity of membrane is related to membrane flux and antifouling ability [24]. The water contact angle measurement showed that the Ba/CaAlg membrane exhibited the inherent superhydrophilicity of hydrogels [4,25,26]. The water contact angle dropped below 10° in just a few seconds. Fig. 2f shows the surface water contact angle of the Ba/CaAlg-1/1, which was only 7.95°. The high hydrophilicity of Ba/CaAlg-1/1 contributed to the improvement of the flux and anti-fouling properties of the membrane.

Combining the mechanical properties and swelling resistance of the Ba/CaAlg membranes, a molar ratio of [Ba^{2+}:Ca^{2+}] = 1:1 was

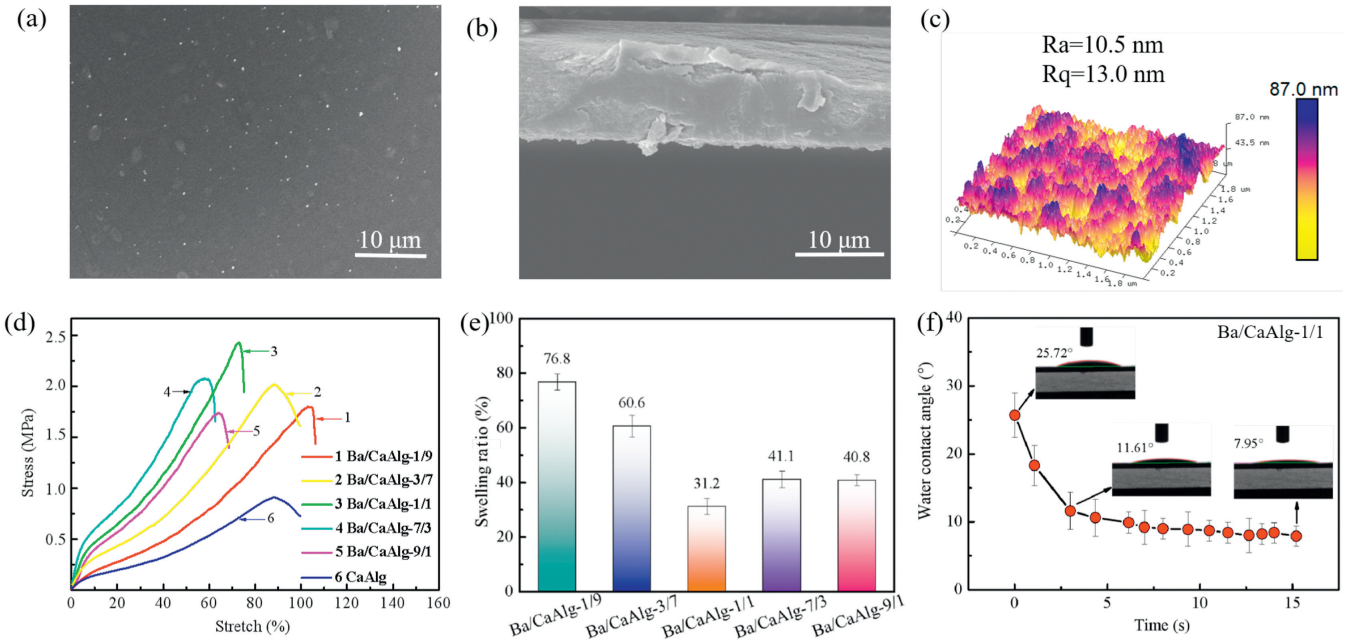

Fig. 2. (a) Surface SEM images of Ba/CaAlg membrane. (b) Cross-sections SEM images of Ba/CaAlg membrane. (c) Surface AFM images of Ba/CaAlg membrane. (d) Stress-strain curves of Ba/CaAlg membranes with different [Ba^{2+}:Ca^{2+}] ratios. (e) Swelling rate of Ba/CaAlg membranes with different [Ba^{2+}:Ca^{2+}] ratios after 2 h in 5.0 g/L NaCl solution. (f) Digital photograph of static equilibrium water contact angle of the Ba/CaAlg-1/1. Data are presented as the mean ± standard deviation (SD) ($n = 3$).

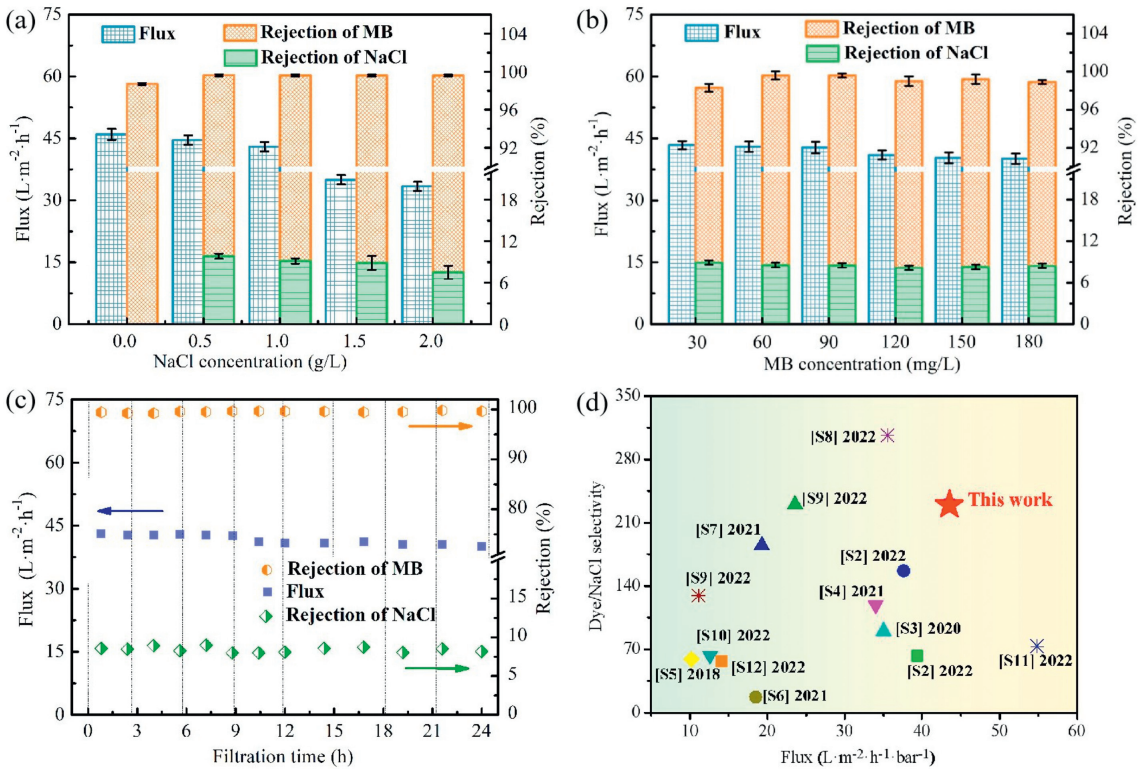

Fig. 3. The effects of NaCl (a) and dye concentration (b) on MB/NaCl separation of Ba/CaAlg-1/1 (0.1 MPa, 25 °C). (c) Continuous separation test of Ba/CaAlg-1/1 on MB/NaCl mixture (NaCl: 1.0 g/L, MB: 60 mg/L, 0.1 MPa, 25 °C). Data are presented as the mean ± SD ($n = 3$). (d) Comparison of the performance of Ba/CaAlg-1/1 with other membranes in the literature for dye/NaCl selective separation (Table S3 in Supporting information). The size information of Na^+, Cl^- and MB was in Tables S1 and S2 (Supporting information).

the optimum formulation of the co-crosslinker, which is consistent with the research results of Fan *et al.* [27]. Considering the stability of gel structure is crucial to the separation process of the membrane, Ba/CaAlg-1/1 was selected for subsequent separation performance test.

The dye/salt separation performance of Ba/CaAlg-1/1 was measured by using methyl blue (MB) and NaCl mixed solution as feed solution. The effect of NaCl concentration on the separation performance is exhibited in Fig. 3a, membrane flux decreased slightly with increasing NaCl concentration. It is worth noting that the re-

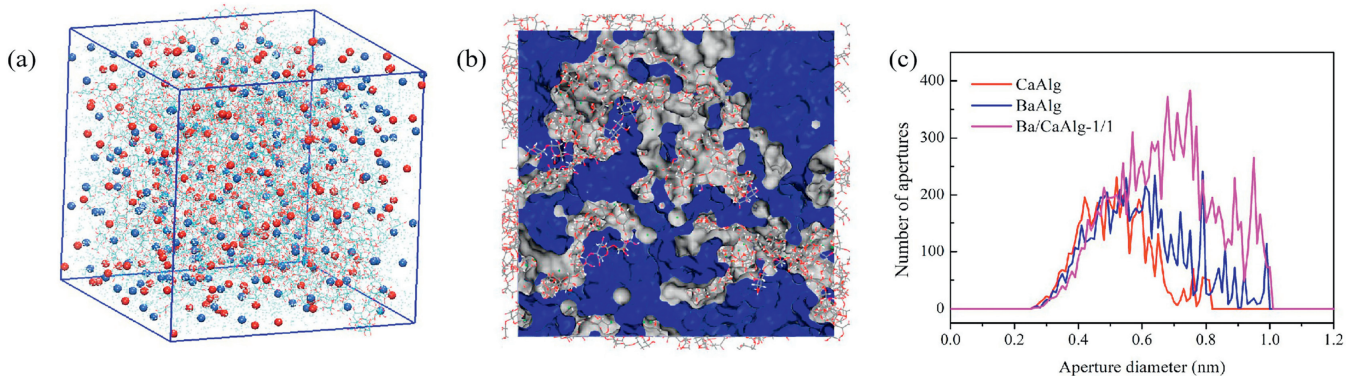

Fig. 4. MD simulation of (a) the microstructure of Ba/CaAlg-1/1 hydrogel, (b) pore structure (red: alginate matrix, white: membrane pore structure, blue: interface pore structure) and (c) pore size distribution of CaAlg, BaAlg and Ba/CaAlg-1/1.

jection of Ba/CaAlg-1/1 for MB was close to 100%, and the rejection for NaCl was low (<10%), realizing the separation of dye/salt. The increase of NaCl concentration enhances the electrostatic shielding effect of Na^+, decreasing the rejection of NaCl, while the low salt rejection reduces the transmembrane pressure difference and limits the permeation driving force [24]. The effect of dye concentration on the separation performance of Ba/CaAlg-1/1 was shown in Fig. 3b. The membrane still maintained a flux of more than 40 $L\,m^{-2}\,h^{-1}$ for MB at a concentration of 180 mg/L, and the rejection of MB (99.6%) and NaCl (8.2%) remained stable. This is attributed to the fact that the energy potential of the hydrophilic membrane surface reduces the deposition or adsorption of dye molecules, thus weakening the effect of concentration polarization on the membrane [24,25]. In addition, the stability of Ba/CaAlg-1/1 was test. Fig. 3c shows that after 24 h continuous separation of MB/NaCl mixed solution, the flux only decreased from 43.5 $L\,m^{-2}\,h^{-1}$ to 40.1 $L\,m^{-2}\,h^{-1}$, and the separation performance of MB and NaCl remained stable.

The dye/salt separation performance of the membranes prepared in this study was compared with other recently reported filtration membranes as shown in Fig. 3d, references and data as displayed in Fig. S3 (Supporting information). It can be seen that the Ba/CaAlg-1/1 exhibited a high selectivity of 229.5 for MB/NaCl. Considering the flux and dye/NaCl separation selectivity synthetically, Ba/CaAlg-1/1 was significantly better than the other alginate hydrogel-based membranes and organic membranes. Moreover, the raw materials used in this work were inexpensive and the preparation process did not involve organic solvent pollution, which is conducive to energy saving and emission reduction as well as large-scale industrial production. Ba/CaAlg membranes have a broad application prospect in the treatment of saline dyeing wastewater and dye recovery.

The microstructure, membrane pore structure and pore size distribution of Ba/CaAlg hydrogel membrane were generated by MD simulation. Details of the MD simulation were provided in Text S2 (Supporting information). The MD results of pore structure for CaAlg and BaAlg were shown in Fig. S1 (Supporting information), and the results of Ba/CaAlg were displayed in Fig. 4. The occupied volume and free volume of BaAlg were 241,975.59 and 58,787.41 $Å^3$, respectively, and the surface area was 98,072.65 $Å^2$. The pore diameter of Ba/CaAlg-1/1 was distributed between 0.6–1.0 nm, which was larger than that of CaAlg and BaAlg. The larger pore diameter demonstrates that the Ba/CaAlg-1/1 membrane has higher flux than BaAlg and CaAlg membranes (Table S3). The MD simulation of transport process, separation mechanisms of dye and salt for CaAlg, BaAlg and Ba/CaAlg membrane is under investigation and the results will be published in a full paper.

In summary, we committed to improve the mechanical strength, stability and membrane flux in salt solutions of alginate hydrogel by co-crosslinking of Ba^{2+} and Ca^{2+} ions. The co-crosslinked structure of hydrogel obtained by crosslinking with the molar ratio of $[Ba^{2+}:Ca^{2+}]=1:1$ was the most stable. At 0.1 MPa pressure, the Ba/CaAlg hydrogel membrane achieved a flux of 43.5 $L\,m^{-2}\,h^{-1}$ for MB/NaCl mixtures with a selection factor of 229.5 for MB/NaCl, which was generally higher than other newly reported membranes and showed good long-term stability.

Declaration of competing interest

The authors declare that they have no known competing financial interests or personal relationships that could have appeared to influence the work reported in this paper.

Acknowledgments

The research is supported by the National Natural Science Foundation of China (No. 22078244), Scientific research and development project of SINOPEC (No. 222443) and the Science and Technology Plans of Tianjin (No. 20JCYBJC00120).

Supplementary materials

Supplementary material associated with this article can be found, in the online version, at doi:10.1016/j.cclet.2023.108820.

References

[1] M. Kamali, D.P. Suhas, M.E. Costa, I. Capela, T.M. Aminabhavi, Chem. Eng. 368 (2019) 474–494.
[2] J. Li, S. Li, X. Wang, et al., Chin. Chem. Lett. 30 (2019) 239–242.
[3] W. Tu, Y. Liu, M. Chen, et al., Chin. Chem. Lett. 34 (2023) 107322.
[4] J.H. Aburabie, T. Puspasari, K.V. Peinemann, J. Membr. Sci. 596 (2020) 117615.
[5] W. Zhao, J. Zhu, J. Hang, W. Zeng, MedComm-Biomater. Appl. 1 (2022) e16.
[6] H. Zimmermann, D. Zimmermann, R. Reuss, et al., J. Mater. Sci. Mater. Med. 16 (2005) 491–501.
[7] R. Fu, H. Zhang, Y. Xie, et al., Mater. Express 12 (2022) 373–377.
[8] H. Ren, Y. Cui, A. Li, D. Qiu, Chin. Chem. Lett. 29 (2018) 395–398.
[9] C. Hu, W. Lu, A. Mata, K. Nishinari, Y. Fang, Int. J. Biol. Macromol. 177 (2021) 578–588.
[10] M.A. Ragan, O. Smidsrød, B. Larsen, Mar. Chem. 7 (1979) 265–271.
[11] K. Zhao, X. Zhang, J. Wei, et al., J. Membr. Sci. 492 (2015) 536–546.
[12] K. Zhao, M. Chen, Y. Zhang, et al., Desalination 538 (2022) 115908.
[13] C. Yue, G. Zhang, J. Environ. Chem. Eng. 10 (2022) 108684.
[14] J. Hu, Y. Chen, J. Lu, et al., Polymer 201 (2020) 122531.
[15] T. Bai, K. Zhao, Z. Lu, et al., Chin. Chem. Lett. 32 (2021) 1051–1054.
[16] W. Xie, K. Zhao, L. Xu, et al., Chin. Chem. Lett. 33 (2022) 1951–1955.
[17] S. Gao, Y. Zhu, J. Wang, et al., Adv. Funct. Mater. 28 (2018) 1801944.
[18] J. Zhang, J. Ke, Y. Zhu, et al., Biomed. Mater. 15 (2019) 015003.

[19] M. Darrabie, W.F. Kendall, E.C. Opara, J. Microencapsul. 23 (2006) 29–37.
[20] G. Reddy, A. Saxena, A. Thakur, Polym. Korea 40 (2016) 63–69.
[21] S. Musa, D. Abu Fara, A. Badwan, J. Control. Release 57 (1999) 223–232.
[22] A.C.K. Bierhalz, M.A. da Silva, M.E.M. Braga, H.J.C. Sousa, T.G. Kieckbusch, LWT 57 (2014) 494–501.
[23] S.K. Bajpai, S. Sharma, React. Funct. Polym. 59 (2004) 129–140.
[24] C.C. Ye, F.Y. Zhao, J.K. Wu, Chem. Eng. J. 307 (2017) 526–536.
[25] Y. Li, S. Sun, J. Indust. Eng. Chem. 114 (2022) 134–141.
[26] Y. Zhang, K. Zhao, Z. Yang, et al., Sep. Purif. Technol. 270 (2021) 118761.
[27] X. Fan, S. Lei, L. Ren, J. Biomed. Eng. 30 (2013) 1272–1275.